Density and pressure profiles for a weakly repulsive Bose gas in a harmonic trap

2007 J. Phys. A: Math. Theor. 40 8665

(http://iopscience.iop.org/1751-8121/40/30/005)

IOP PUBLISHING JOURNAL OF PHYSICS A: MATHEMATICAL AND THEORETICAL

J. Phys. A: Math. Theor. **40** (2007) 8665–8681 doi:10.1088/1751-8113/40/30/005

Density and pressure profiles for a weakly repulsive Bose gas in a harmonic trap

Sonia Lumb and S K Muthu

Department of Physics and Astrophysics, University of Delhi, Delhi-110 007, India

E-mail: skmuthu@physics.du.ac.in

Received 23 April 2007, in final form 11 June 2007
Published 12 July 2007
Online at stacks.iop.org/JPhysA/40/8665

Abstract

A simple numerical scheme based on the local equilibrium theory is developed to compute the density and pressure profiles of a weakly repulsive Bogoliubov gas. From these profiles the local velocity of sound has been calculated. The numerical scheme avoids the divergence problems encountered in some cases and the results agree well with those of previous workers. The effect of interactions on bosons confined to a small region of space by a bounded harmonic potential of extent r_0 has also been studied.

PACS numbers: 21.60.Fw, 05.30.Jp, 03.75.Hh

1. Introduction

The characteristics of BEC are significantly altered by the interatomic interactions, particularly when the condensation density becomes a sizeable fraction of the total density at low temperatures. The model generally employed is that of a weakly repulsive dilute Bose gas which has been extensively studied by a number of authors. The path-breaking work of Bogoliubov [1] was followed by Huang, Yang and Luttinger extending the theory to non-zero temperatures using the pseudopotential method [2]. The application of field-theoretic methods to this problem was initiated by Beliaev [3] and extended by Popov among others [4, 5]. However, the fully microscopic approaches, referred to above, are not easily adaptable to systems which are of finite extent or which are inhomogeneous in other ways.

A very fruitful idea of the condensate wavefunction $\psi(r)$ as the 'order parameter' was introduced independently by Gross and Pitaevskii [6, 7] who derived a differential equation for $\psi(r)$, now known as the Gross–Pitaevskii (GP) equation. This equation, analogous to the Ginzburg–Landau (GL) equation for superconductors, has been applied with great success to the problem of trapped Bose condensates [8–10].

We employ the local equilibrium theory to study the properties of a weakly repulsive Bose gas in a harmonic potential. Detailed calculations of the various thermodynamic functions

are available [10, 11]. Many of these approaches employ perturbation expansions, which are plagued by divergences in the vicinity of the critical temperature T_C [12]. Hence, it is difficult to set up a meaningful approximation scheme. The density profile of the weakly interacting Bose gas confined in a potential well has been calculated by Oliva [13] and Su *et al* [14] using the local equilibrium theory. Oliva breaks up the density into four intervals for calculating the chemical potential and employs a very tedious scheme to carry out the calculations. Su *et al* [14] resort to perturbation expansions which also lead to very complicated expressions and need to be handled carefully in the degenerate phase.

We discuss the formulation of the problem in section 2 and develop a consistent numerical scheme, avoiding any perturbation expansions. The degenerate and the non-degenerate phases are treated separately in sections 3.1 and 3.2, respectively. A major difference, compared to the homogeneous case, is the appearance of a surface of separation between the degenerate and the non-degenerate phases. We make a numerical estimate of the radius x_D of this surface. This enables us to calculate the density and pressure profiles and the local sound velocity. Some independent checks on the numerical calculations are discussed in section 3.3.

The potential employed in our calculations is the usual unbounded harmonic potential extending to infinity. However, it is of interest to study particles confined in a finite trap of size r_0. Lumb and Muthu [19, 21] and Lumb *et al* [15] have studied BEC and the thermodynamic properties of a system of non-interacting trapped bosons, using the bounded harmonic potential (BHP) which extends to r_0 rather than infinity.

The interplay of a finite size and interactions is also worthy of study and can lead to interesting possibilities. We content ourselves by reporting the calculations for one typical case in section 3.4. A discussion of the results and our main conclusions is presented in section 4.

2. Formulation of the problem: density and pressure profiles

We consider a system of N bosons, each of mass m, under the effect of an isotropic harmonic potential, typical of experimental traps. The potential has the form

$$V(r) = \tfrac{1}{2}m\omega^2 r^2, \tag{1}$$

ω being the confining oscillator frequency. The generalization to anisotropic harmonic traps is straightforward. The system is supposed to be divided into small cubical cells of size L^3. For each cell the external potential is taken to be constant equal to its value at the centre of the cell. The cells are such that the number of bosons in each cell is large enough for them to be treated as a Bose gas in a uniform averaged potential. We also assume these cells to be statistically independent of one another but in mutual equilibrium. For equilibrium, the chemical potential of the cells has to be a constant and it is given by the sum of the local internal chemical potential and the applied external potential, i.e.

$$\mu = \mu_{\rm int}(\boldsymbol{r}) + V_{\rm ext}(\boldsymbol{r}). \tag{2}$$

The internal chemical potential within a cell is the chemical potential of a field-free Bose gas which is a functional of its local density, i.e.

$$\mu_{\rm int}(\boldsymbol{r}) = \mu^{\rm FF}(n(\boldsymbol{r})). \tag{3}$$

This lattice equilibrium theory is discussed in detail by Lumb *et al* [15].

We consider a sufficiently dilute gas, so that only binary collisions are relevant and these collisions are characterized by a single parameter, namely the s-wave scattering length 'a'. The two-body potential can be written as

$$V(\boldsymbol{r}) = v_0\delta(\boldsymbol{r})\frac{\partial}{\partial r}r, \qquad r = |\boldsymbol{r_1} - \boldsymbol{r_2}|, \tag{4}$$

where the coupling constant v_0 is related to 'a' through

$$v_0 = \frac{4\pi\hbar^2 a}{m}. \tag{5}$$

For a wavefunction $\psi(\boldsymbol{r})$, (4) gives

$$V(\boldsymbol{r})\psi(\boldsymbol{r}) = v_0\delta(\boldsymbol{r})\frac{\partial}{\partial r}(r\psi(\boldsymbol{r})). \tag{6}$$

If $\psi(\boldsymbol{r})$ is regular in $\boldsymbol{r} = \mathbf{o}$, it yields the usual expression

$$V(\boldsymbol{r})\psi(\boldsymbol{r}) = v_0\psi(\mathbf{o})\delta(\boldsymbol{r}). \tag{7}$$

The parameter (na^3) should be $\ll 1$ in the dilute limit. This is satisfied by all alkali gas condensates. To extend the theory to the case of a weakly repulsive Bose gas, all one has to do is to replace the ideal Bose gas in each cell by the corresponding Bogoliubov weakly interacting gas. It is well known that for a field-free Bogoliubov gas below the critical temperature T_C of BE transition, not very far from T_C, the chemical potential can be written as [16]

$$\mu^{FF}(n(\boldsymbol{r})) = n^{FF}(\boldsymbol{r})v_0 + n_C(T)v_0, \tag{8}$$

where $n(\mathbf{r})$ is the density of the gas,

$$n_C(T) = \frac{2.612}{\lambda^3} \tag{9}$$

is the critical density, i.e. the density at the onset of BEC and λ is the thermal de-Broglie wavelength of the particles of mass m at temperature T given by

$$\lambda = \left\{\frac{h}{\sqrt{2\pi mkT}}\right\}. \tag{10}$$

The thermodynamic potential $\Omega(m)$ of the gas in a cell centred at m with a uniform potential $V(\mathbf{r}_m)$ is

$$\Omega(m) = -\frac{1}{\beta}\ln \mathrm{Tr}\left\{\exp\left[-\beta\left(\sum_{\mathbf{k}}\left(\frac{\hbar^2k^2}{2m} - (\mu - V(\mathbf{r}_m))\right)a_k^\dagger a_k + V_{\mathrm{int}}\right)\right]\right\}, \tag{11}$$

where

$$V_{\mathrm{int}} = \frac{v_0}{2v}\sum_{k_1,k_2,k_3} a_{k_1}^\dagger a_{k_2}^\dagger a_{k_3}a_{k_1+k_2-k_3}, \tag{12}$$

v is the volume of a cell, a_k, $a_k^\dagger$ denote, respectively, the annihilation and creation operators of particles in the cell m and the wave vectors $\mathbf{k}$ of the particles are given by

$$\boldsymbol{k} = \frac{2\pi}{L}(n_1, n_2, n_3), \qquad n_i = 0, \pm1, \pm2, \ldots. \tag{13}$$

Equation (11) for Ω is the same as that of a gas in zero external potential with chemical potential $\mu' = \mu - V(\mathbf{r}_m)$. The pressure is given by the usual thermodynamic relation

$$P(m) = -\left.\frac{\partial\Omega(m)}{\partial v}\right|_{T,\mu}. \tag{14}$$

Since v remains unaltered by the application of an external potential we can obtain P by just replacing the internal chemical potential by μ' in the expression [16]

$$P^{FF} = \frac{kT}{\lambda^3}\zeta(5/2) + \frac{v_0}{2}\left\{[n^{FF}]^2 + n_C^2(T)\right\}. \tag{15}$$

Since μ appears only in the expression for the density we need to first derive an expression for the density.

The average number of particles in a cell, $\bar{N}_{\rm cell}$, is given as

$$\bar{N}_{\rm cell} = -\left.\frac{\partial\Omega(m)}{\partial\mu}\right|_{T,v} = -\left.\frac{\partial\Omega^{\rm FF}(\mu')}{\partial[\mu^{\rm FF}+V(\boldsymbol{r}_{\rm m})]}\right|_{T,v} = -\left.\frac{\partial\Omega^{\rm FF}(\mu')}{\partial\mu^{\rm FF}}\right|_{T,v} = \bar{N}^{\rm FF}(\mu'). \tag{16}$$

Hence, we only need to use the displaced chemical potential. The same, obviously, is true for the density, i.e.,

$$\bar{n}_{\rm cell}(\boldsymbol{r}_{\rm m}) = \bar{n}^{\rm FF}(\mu', T). \tag{17}$$

From (8), it follows that

$$\bar{n}_{\rm cell}(\boldsymbol{r}_{\rm m}) = [\mu - V(\boldsymbol{r}_{\rm m}) - n_{\rm C}(T)v_0]/v_0. \tag{18}$$

The same is true for the condensate density, namely

$$n_0^{\rm FF} = n^{\rm FF} - n_{\rm C}(T), \tag{19}$$

and hence

$$n_0(\boldsymbol{r}_{\rm m}) = [\mu - V(\boldsymbol{r}_{\rm m}) - 2n_{\rm C}(T)v_0]/v_0. \tag{20}$$

This is an important relation since it furnishes an equation for the surface separating the degenerate and the normal phases. Let the radius of the degenerate phase be given by $r_{\rm D}$. Then $n_0(r_{\rm D}) = 0$ gives

$$\tfrac{1}{2}m\omega^2 r_{\rm D}^2 = \mu - 2n_{\rm C}(T)v_0. \tag{21}$$

The number of particles in the degenerate phase is obtained by integrating $\{n_0 + n_{\rm C}(T)\}$ over the region extending from 0 to $r_{\rm D}$. This yields

$$N_{\rm deg} = \frac{2}{3\sqrt{2\pi}}\zeta(3/2)\tau^{3/2}x_{\rm D}^{3/2} + \frac{x_{\rm D}^{5/2}a_0}{15a}, \tag{22}$$

where

$$x_{\rm D} = \left(\frac{r_{\rm D}}{a_0}\right)^2, \tag{23}$$

$$\tau = \frac{kT}{\hbar\omega} \tag{24}$$

is the dimensionless temperature and

$$a_0 = \left(\frac{\hbar}{m\omega}\right)^{1/2} \tag{25}$$

is the harmonic oscillator length. $T_{\rm C}$, the critical temperature of BEC phase transition is the temperature for which the degenerate phase radius $r_{\rm D}$ shrinks to zero. Therefore $r_{\rm D} = 0$ gives the critical line of the system. We have from (21)

$$\mu_{\rm C} = 2n_{\rm C}(T)v_0, \tag{26}$$

where $\mu_{\rm C}$ is the critical chemical potential.

For the normal part, or the non-degenerate phase, $r > r_{\rm D}$ and [16]

$$\mu^{\rm FF} = \mu_0 + 2n^{\rm FF}v_0, \tag{27}$$

μ_0 being the chemical potential of the uniform ideal Bose gas. The density of the particles in the excited states is given by

$$n = \frac{1}{\lambda^3}g_{3/2}[\exp(\beta\mu_0)], \tag{28}$$

$g_r(z)$ being the Bose–Einstein functions defined by

$$g_r(z) = \frac{1}{\Gamma(r)} \int_0^\infty \frac{x^{r-1}\,dx}{z^{-1}\,e^x - 1} = \sum_{l=1}^{\infty} \frac{z^l}{l^r}. \tag{29}$$

Replacing μ^{FF} by μ' and substituting for μ_0 from (27), we have

$$n(\boldsymbol{r}_m) = \frac{1}{\lambda^3} g_{3/2}\{\exp[\beta(\mu' - 2n(\boldsymbol{r}_m)v_0)]\}. \tag{30}$$

This is a transcendental equation and needs to be solved numerically. Writing it in terms of $x = (r/a_0)^2$ and τ and using (21), we get

$$n(\boldsymbol{r}_m)\lambda^3 = g_{3/2}\left(\exp\left\{-\left[\frac{x - x_D}{2\tau} - \eta(2.612 - n(\boldsymbol{r}_m)\lambda^3)\right]\right\}\right) \tag{31}$$

with

$$\eta = 2\sqrt{\frac{2\tau}{\pi}}\frac{a}{a_0} \approx 1.6\tau^{1/2}\frac{a}{a_0}. \tag{32}$$

If we put $a(x) = 2.612 - n(\boldsymbol{r}_m)\lambda^3$, (31) becomes

$$2.612 - a(x) = g_{3/2}\left\{\exp\left[-\left(\frac{x - x_D}{2\tau} - \eta a(x)\right)\right]\right\} \tag{33}$$

and

$$n^{\text{non-deg}}(\boldsymbol{r}_m) = \frac{2.612 - a(x)}{\lambda^3}. \tag{34}$$

The number of particles in the non-degenerate phase is given by integrating (34) with r ranging from r_D to some maximum value r_0 or equivalently x ranging from x_D to x_0.

$$N_{\text{non-deg}} = \frac{\tau^{3/2}}{\sqrt{2\pi}} \int_{x_D}^{x_0} [2.612 - a(x)]x^{1/2}\,dx. \tag{35}$$

The choice of x_0 is dictated by the desired accuracy. The total number of particles for $T < T_C$ is given by the sum of (22) and (35). The number density in the degenerate cells is obtained from (18) and (21) as

$$n^{\text{deg}}(\boldsymbol{r}_m)a_0^3 = \frac{\zeta(3/2)\tau^{3/2}}{(2\pi)^{3/2}} + \frac{(x_D - x)a_0}{8\pi a} \tag{36}$$

and the contribution to the pressure from the degenerate cells can now be written as

$$\frac{P_{\text{cell}}^{\text{deg}}a_0^3}{\hbar\omega} = \frac{\tau^{5/2}\zeta(5/2)}{(2\pi)^{3/2}} + \frac{\tau^3\zeta^2(3/2)a}{2\pi^2 a_0} + \frac{(x_D - x)^2 a_0}{32\pi a} + \frac{\zeta(3/2)\tau^{3/2}(x_D - x)}{2(2\pi)^{3/2}}. \tag{37}$$

For non-degenerate cells the pressure is given by

$$P^{\text{non-deg}}(m) = \frac{kT}{\lambda^3} g_{5/2}[\exp(\beta\mu_0)] + v_0 n^2(\boldsymbol{r}_m) \tag{38}$$

or

$$\frac{P_{\text{cell}}^{\text{non-deg}}a_0^3}{\hbar\omega} = \frac{\tau^{5/2}}{(2\pi)^{3/2}} g_{5/2}\left(\exp\left\{-\left[\frac{(x - x_D)}{2\tau} - \eta a(x)\right]\right\}\right) + \frac{\tau^3 a}{2\pi^2 a_0}[2.612 - a(x)]^2. \tag{39}$$

For $T > T_C, r_D = 0$. We again use (30) and the range of integration now extends from zero to some maximum value x_0. We now proceed to outline a numerical scheme to carry out the calculations.

3. Numerical scheme

3.1. Degenerate phase

The scheme consists in fixing the total number of particles N and the interaction strength 'a' in terms of the harmonic oscillator length a_0. We have taken two cases, namely (i) $N = 10\,000, a = 10^{-3}a_0$ and (ii) $N = 40\,000, a = 110a_B$ with $\omega = 1171.815(s^{-1})$, a_B being the Bohr radius. We choose ω in the second case as the geometric average of ω_x, ω_y and ω_z used by Su *et al* [14]. Next for some given value of τ, for which the profiles are to be plotted, we choose some value of r_D in terms of a_0. Note that the smallest possible cell size for an ideal gas is $\sqrt{2\pi}a_0$ [15]. We solve for $a(x)$ in (33) using the method of inverse interpolation. From this we calculate the total number of particles as the sum of (22) and (35). The calculations are repeated for some other values of r_D and the value corresponding to fixed N is determined graphically. Inverse interpolation is used as a check on this value. The corresponding x_D is calculated from (23), and (34), (36), (37) and (39) are used for plotting of profiles for this temperature. The exercise is repeated for a range of values of $\tau (10 \leqslant \tau < \tau_C)$.

3.2. Non-degenerate phase

We write (30) as

$$b(x) = g_{3/2}\left[\exp\left(\frac{\mu}{\hbar\omega\tau} - \frac{x}{2\tau} - \eta b(x)\right)\right], \tag{40}$$

where

$$n^{\text{non-deg}}(\boldsymbol{r}_m) = \frac{b(x)}{\lambda^3}. \tag{41}$$

Pressure is now given as

$$\frac{P_{\text{cell}}^{\text{non-deg}} a_0^3}{\hbar\omega} = \frac{\tau^{5/2}}{(2\pi)^{3/2}} g_{5/2}\left[\exp\left(\frac{\mu}{\hbar\omega\tau} - \frac{x}{2\tau} - \eta b(x)\right)\right] + \frac{\tau^3 a}{2\pi^2 a_0} b(x)^2. \tag{42}$$

The self-consistent procedure for performing the calculations parallels the one used above for the degenerate phase and consists of the following sequence of steps:

(i) We fix the values of N and (a/a_0).
(ii) We fix τ and choose some starting value of $|\mu|/\hbar\omega$. Next (40) is solved for $b(x)$ using Bessel's formula of inverse interpolation, varying x in steps of 0.01.
(iii) The total number of particles is obtained by integrating (41). The whole process is repeated for a set of values of $|\mu|/\hbar\omega$. A graph is plotted between N and $|\mu|/\hbar\omega$. For the sake of illustration, we give the graph for $\tau = 30, a/a_0 = 10^{-3}$ in figure 1.
(iv) The value of $|\mu|/\hbar\omega$ corresponding to a given N is read from the graph and N is again calculated using (41).
(v) The whole process is repeated till we get a value of N which differs from the desired value by less than a few parts in 10^5. For example, from the graph of figure 1, we get $|\mu|/\hbar\omega = 31.126$ for $N = 10^4$.

Once $\mu/\hbar\omega$ is known, we can plot both density and pressure profiles using (41) and (42). These plots are shown in figures 2–5.

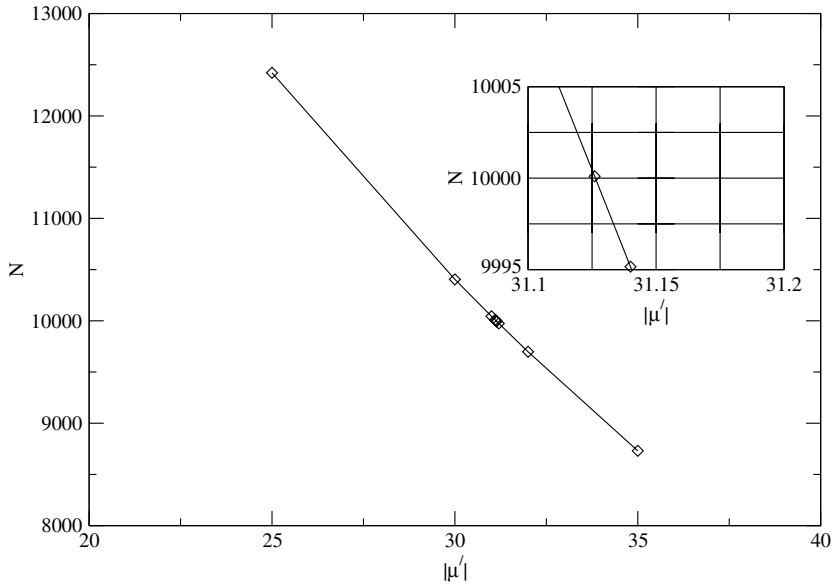

Figure 1. Graph for finding $|\mu|/\hbar\omega$ for $N = 10\,000$ and $a/a_0 = 0.001$ at $\tau = 30$.

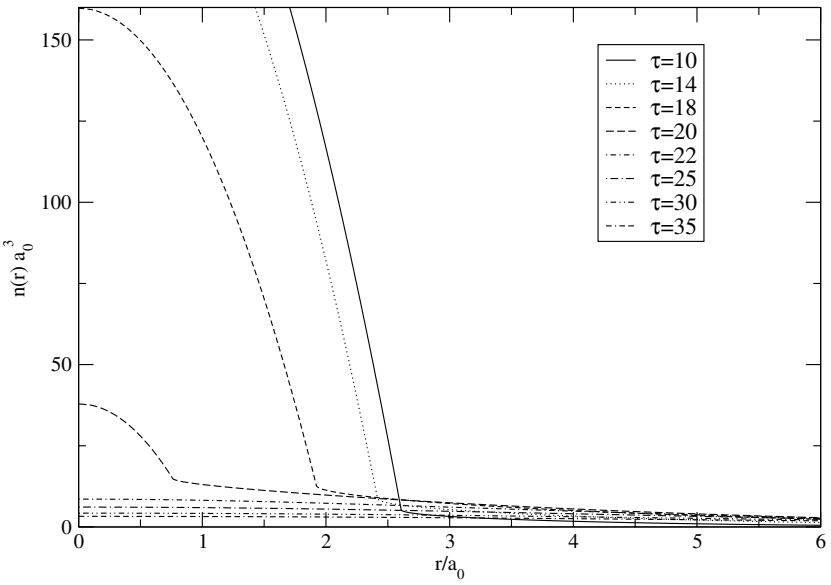

Figure 2. Density profiles for $N = 10\,000$ and $a/a_0 = 0.001$.

3.3. Some independent checks on the numerical computations

3.3.1. Comparison with Su et al [14]. As pointed out in section 1, the various perturbation schemes, if not carefully used, fail to converge in the degenerate phase [12]. However, as a check on our calculations, we can compare our results with Su *et al* [14] in the non-degenerate phase. To this end, we need to estimate $\tilde{z} = \exp(\beta\mu_0(0))$, the non-interacting internal fugacity

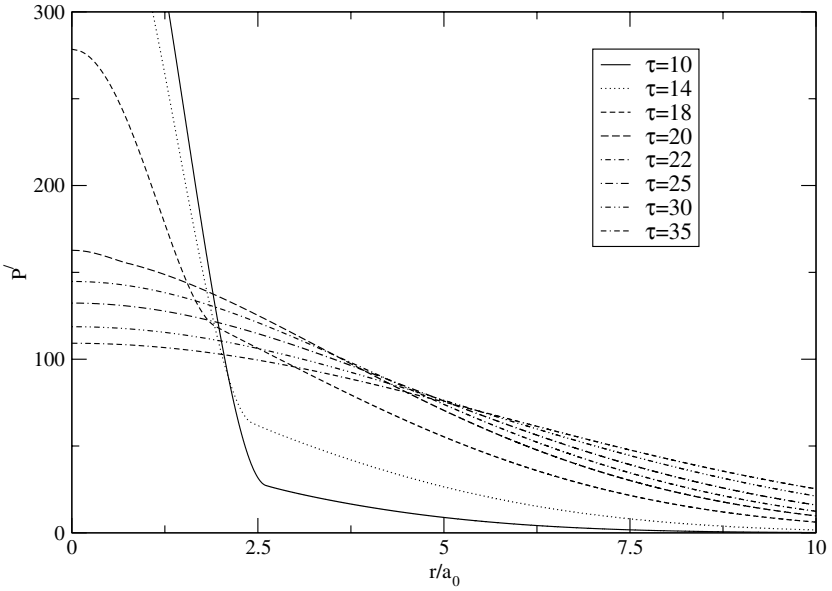

Figure 3. Pressure profiles for $N = 10\,000$ and $a/a_0 = 0.001$.

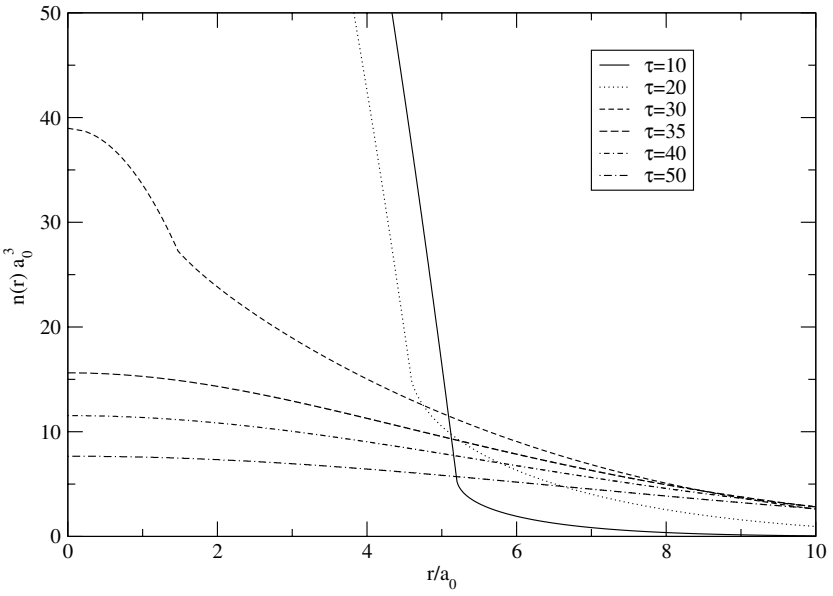

Figure 4. Density profiles for $N = 40\,000$ and $a/a_0 \approx 0.007$.

at the centre of the potential. Chou, Yang and Yu [17] derive an explicit expression for $n_0(\boldsymbol{r})$ by calculating the density matrix. Their result is

$$n_0(\boldsymbol{r})\lambda^3 = \frac{1}{\tau^{3/2}} \sum_{l=1}^{\infty} \left(\sinh \frac{l}{\tau} \right)^{-3/2} z^l \exp\left[-\frac{r^2}{a_0^2} \tanh\left(\frac{l}{2\tau} \right) \right]. \tag{43}$$

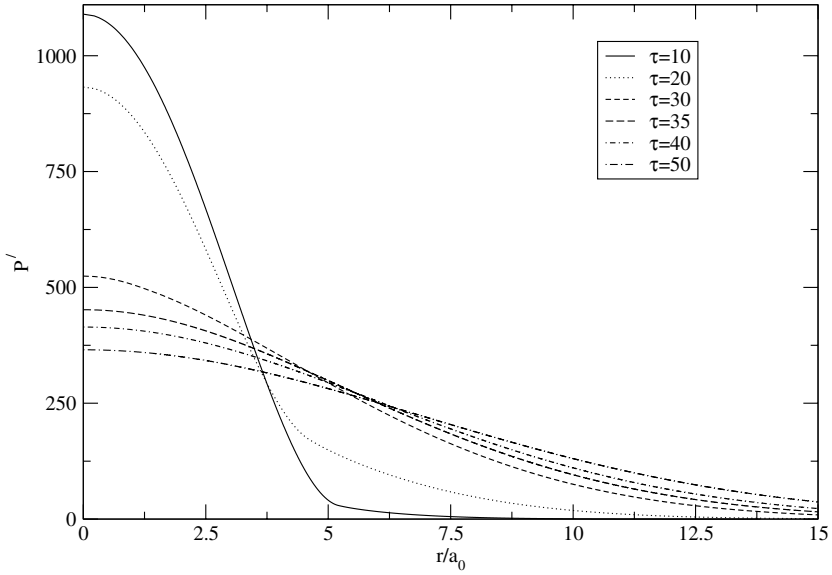

Figure 5. Pressure profiles for $N = 40\,000$ and $a/a_0 \approx 0.007$.

Table 1. Comparison of fugacity values.

τ	Numerical method	Analytical method of Su *et al* [14]
	$N = 40\,000$, $a/a_0 \approx 0.007$	
35.0	0.842	0.817
40.0	0.586	0.574
50.0	0.311	0.307

From this one obtains

$$n_0(\mathbf{o})\lambda^3 = \frac{1}{\tau^{3/2}} \sum_{l=1}^{\infty} \left(\sinh \frac{l}{\tau} \right)^{-3/2} z^l. \tag{44}$$

Integrating (43) over $\mathbf{r}$ gives

$$N = \frac{1}{8} \sum_{l=1}^{\infty} \frac{z^l}{\left(\sinh^3 \frac{l}{2\tau} \right)}. \tag{45}$$

Fixing N and τ we can obtain z from this equation. Using (13) of Su *et al* [14]

$$\ln z = \ln \tilde{z} + \eta n_0(0)\lambda^3 \tag{46}$$

with η given by (32), we can estimate $\tilde{z}$ using (44). This $\tilde{z}$ can be plugged into (14) of Su *et al* [14] to obtain $n(\boldsymbol{r})$. For a comparison of the numerical results with the analytical method we choose the values of fugacity z. These are given in table 1.

We have also plotted the density profiles for these temperatures by the two methods. These are shown in figure 6.

3.3.2. Calculation of T_C. We have estimated τ_C by locating the point $x_D = 0$ on the temperature axis of the x_D–τ plot. These plots are shown in figures 7 and 8. We can also use

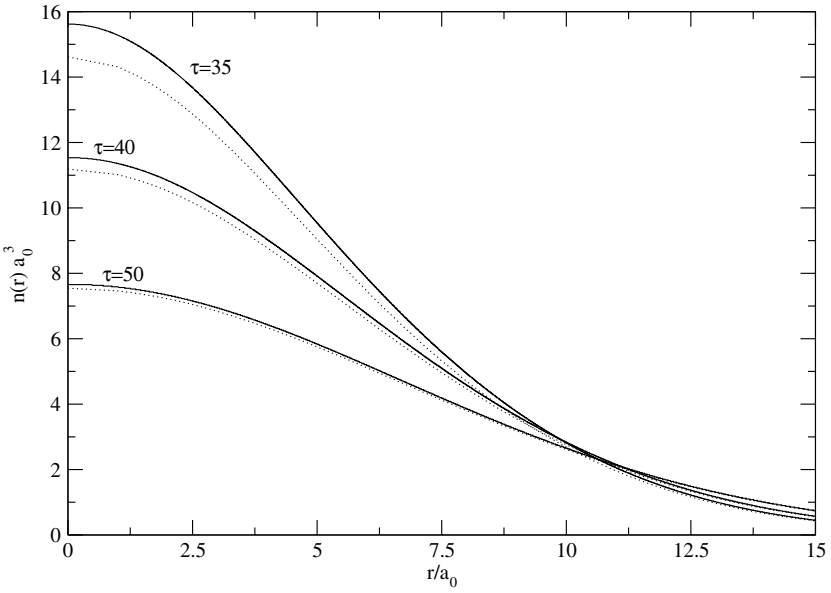

Figure 6. Comparison of density profiles for $N = 40\,000$ and $a/a_0 \approx 0.007$ by numerical method and using (14) of [14]. The solid line represents the results of our numerical method and the dotted line shows the results of analytical method, i.e. using (14) of [14].

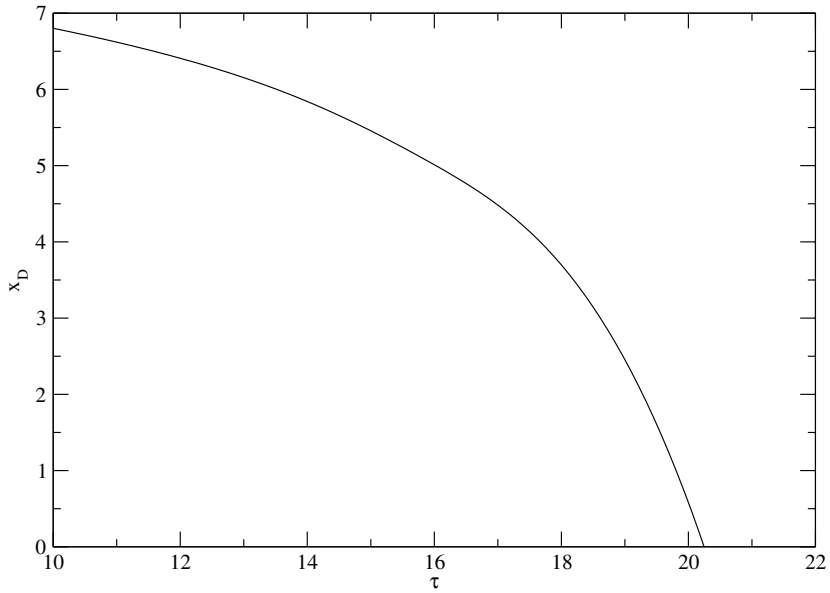

Figure 7. Condensate radius x_D versus τ for $N = 10\,000$ and $a/a_0 = 0.001$.

the condition for the critical line, given by (26), to get an estimate of τ_C. Using this value of μ we calculate the number density using (40) and (41) and hence, the total number of particles, for various τ values. The value of τ corresponding to a given fixed N is then found graphically. This τ is then called the critical temperature τ_C.

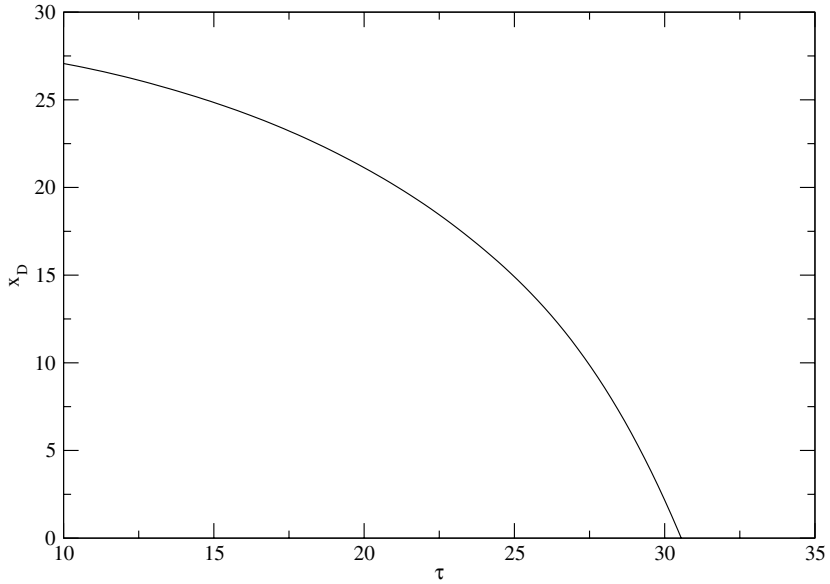

Figure 8. Condensate radius x_D versus τ for $N = 40\,000$ and $a/a_0 \approx 0.007$.

Table 2. Comparison of τ_C values.

	From $x_D = 0$	Using (26)	Kao and Jiang [18]
		(a) $N = 40\,000$, $a/a_0 \approx 0.007$	
τ_C	30.6	35.1	29.7
		(b) $N = 10\,000$, $a/a_0 = 0.001$	
τ_C	20.4	20.5	20.1

In a recent paper Kao and Jiang [18] made a calculation of T_C for a trapped weakly interacting Bose gas taking the contributions of both the thermal and condensate components into account. They obtained the result

$$\frac{T_C}{T_C^0} = 1 - 1.78\frac{a}{a_0}N^{1/6} \tag{47}$$

with

$$T_C^0 \approx 0.9405\frac{\hbar\omega}{k}N^{1/3}. \tag{48}$$

The comparison of the results of the three methods is given in table 2.

3.4. The bounded harmonic oscillator potential (BHP) case

As pointed out in the introduction the combined effect of a finite size and interactions can lead to interesting possibilities. So we now look at such a system. To this end, we have to adapt the calculations of section 3.3 to the case of a BHP.

For reasons outlined in the introduction, we define

$$\begin{aligned} V(r) &= \tfrac{1}{2}m\omega^2 r^2, & r < r_0 \\ &= \infty, & r > r_0 \end{aligned} \tag{49}$$

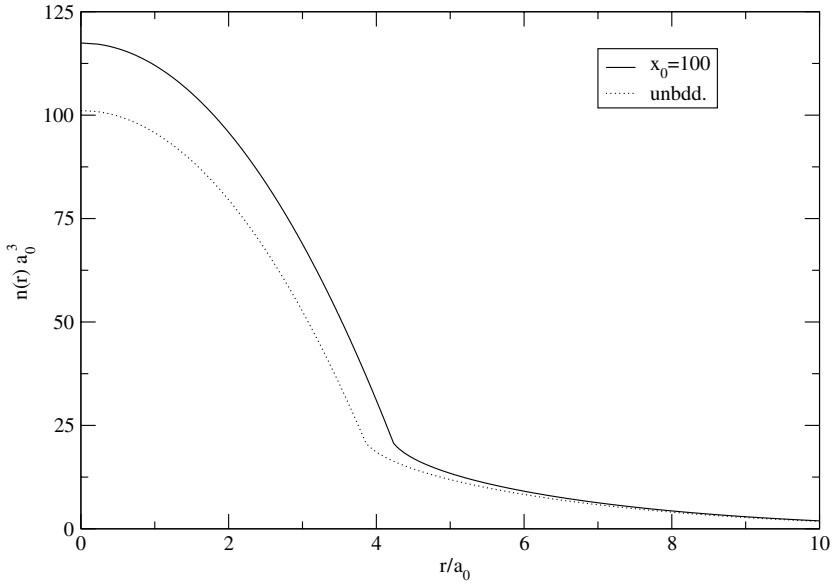

Figure 9. Density profiles for $N = 40\,000, a/a_0 \approx 0.007, \tau = 25$; $x_0 = 100$ and for an unbounded potential.

and call it the bounded harmonic potential (BHP). In the limit $r_0 \to \infty$, it becomes identical with the unbounded harmonic potential. A detailed argument for this choice was given by us in an earlier publication [15]. Here, we outline the essence of the argument.

If the highest energy level, E_{m}, that matters at a certain temperature is $V(r_0)/\alpha$, with α say about 2, the particles are essentially bound in the region $r < r_0$. Coupled with the condition of the applicability of statistical mechanics, namely $E_{\mathrm{m}} \gg kT$, one obtains the condition

$$\frac{a_1}{\alpha} \gg 1 \tag{50}$$

with

$$a_1 = \frac{x_0}{2\tau}, \qquad x_0 = \frac{r_0^2}{a_0^2}. \tag{51}$$

a_1, which can also be written as $V(r_0)/kT$, serves as a cross-over parameter [19]. For $a_1 \to 0$ we have the limit of a uniform ideal gas while $a_1 \to \infty$ represents bosons in an unbounded harmonic potential. It has been shown in [15] that finite-size effects become appreciable for approximately $2 \leqslant a_1 \leqslant 7$.

To illustrate the general principles involved we shall fix $x_0 = 100$ and $\tau = 25$, so that $a_1 = 2$. The numerical scheme outlined in section 3.3 will still work. However, in the present case, the value of x_0 is fixed by the size of the trap and is not dictated by the desired accuracy. We fix N and a/a_0 as before. Then we calculate x_{D} for various values of τ. Substituting these into the relevant formulae we can plot the density and pressure profiles. We can compare these profiles with those plotted for an unbounded harmonic oscillator potential for the case of $N = 40\,000$ and $a/a_0 \approx 0.007$. The comparison is shown in figures 9 and 10.

The density and pressure profiles can be used to calculate the local velocity of sound c via the relation

$$c^2 = \frac{1}{m}\left(\frac{\partial P}{\partial n}\right) = a_0^2\omega^2\left(\frac{\partial P'}{\partial\left(na_0^3\right)}\right). \tag{52}$$

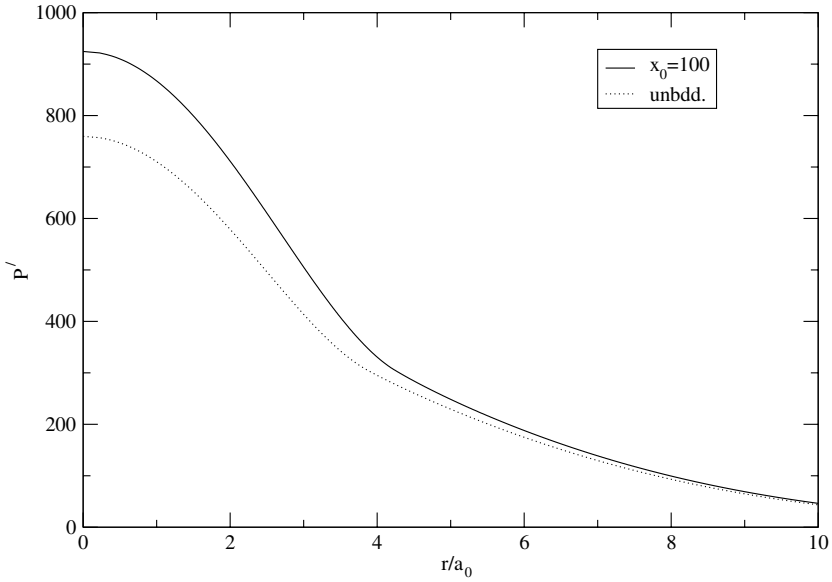

Figure 10. Pressure profiles for $N = 40\,000, a/a_0 \approx 0.007, \tau = 25$; $x_0 = 100$ and for an unbounded potential.

Table 3. Comparison of dimensionless velocity of sound.

x	Unbounded	Bounded ($x_0 = 100$)
$N = 40\,000, a/a_0 \approx 0.007, \tau = 25$		
1.0	3.052	3.290
2.0	2.892	3.143
5.0	2.620	2.894

We give the values for the dimensionless velocity of sound $c/(a_0\omega)$ for $N = 40\,000, a/a_0 \approx 0.007$, for $\tau = 25$ for both the unbounded potential and the BHP in table 3. A graph depicting its variation with the distance from the centre of the trap for both the unbounded and BHP at $\tau = 25$ is shown in figure 11. The density and pressure profiles can also be used to work out the local isotherms and the local equations of state.

We have also plotted the condensate fraction for $N = 40\,000$ for both the ideal and the interacting gases ($a/a_0 \approx 0.007$) for $x_0 = 100$, and for the infinitely extended harmonic potential, in figure 12.

4. Results and conclusions

In the preceding sections we have employed the local equilibrium theory to study the properties of a weakly repulsive Bose gas in a harmonic potential. For this all one has to do is to replace the ideal Bose gas in each cell by the corresponding Bogoliubov weakly interacting gas in the scheme adopted by Lumb *et al* [15].

A consistent numerical scheme, developed in section 3, enables us to make an estimate of the radius x_D of the surface of separation between the degenerate and the non-degenerate phases. Armed with this knowledge, we are able to calculate the density and pressure profiles

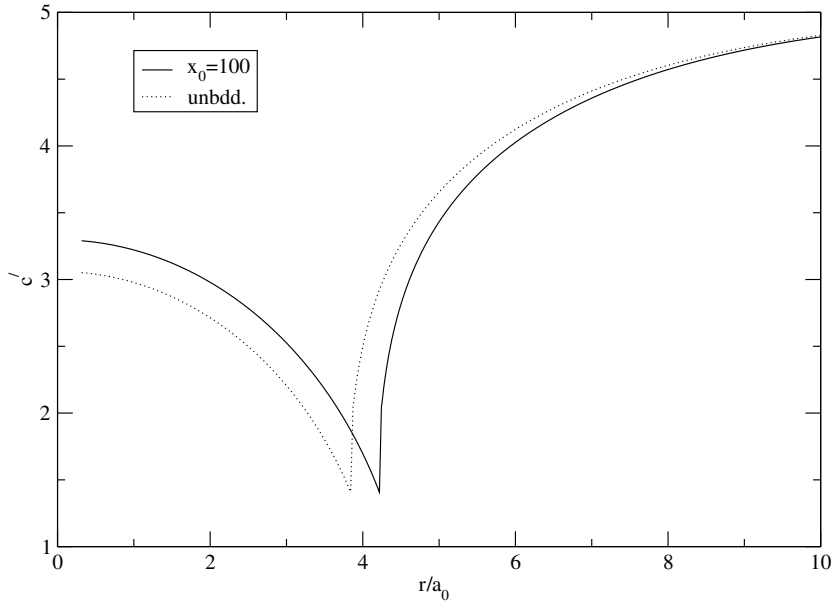

Figure 11. Comparison of dimensionless velocity of first sound for $N = 40\,000$ for weakly repulsive ($a/a_0 \approx 0.007$) gas in an unbounded oscillator potential as well as a bounded potential corresponding to $x_0 = 100$ for $\tau = 25$.

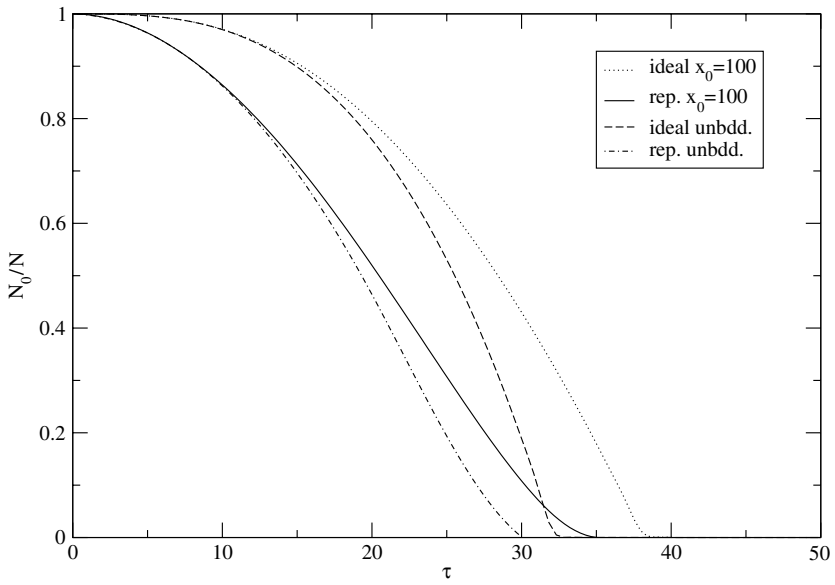

Figure 12. Comparison of condensate fraction N_0 for $N = 40\,000$ for ideal and weakly repulsive ($a/a_0 \approx 0.007$) gas in a bounded potential corresponding to $x_0 = 100$.

for a fixed (i) total number of particles N and (ii) a/a_0, for various values of τ. This entails, inter-alia, solving (33) and (40), using the method of inverse interpolation. The profiles are calculated using (34), (36), (37) and (39). These plots are shown in figures 2–5. Figure 2

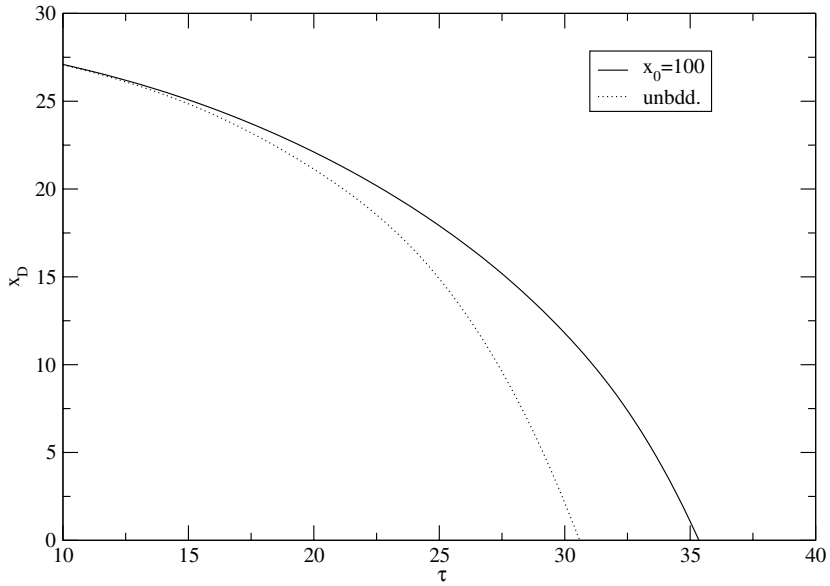

Figure 13. Comparison of x_D for the unbounded potential and the BHP corresponding to $x_0 = 100$ for $N = 40\,000$ ($a/a_0 \approx 0.007$).

depicts the density profile, showing the behaviour of $n(r)a_0^3$ as a function of r/a_0, for $N = 10^4$ and $a/a_0 = 0.001$, for a range of values of $\tau(10 \leqslant \tau \leqslant 35)$. The calculated τ_C is close to 20 (table 2). Note the pronounced enhancement in $n(r)a_0^3$ for $\tau = 20$ near $r/a_0 \approx 0.75$. In figure 4 we plot the density profile for the case $N = 40\,000$ and $a/a_0 \approx 0.007$, for $(10 \leqslant \tau \leqslant 50)$. The enhancement near τ_C for $r/a_0 \approx 1$ is again evident. Our approximation scheme avoids all convergence problems associated with perturbation expansions close to τ_C.

Figures 3 and 5 give the corresponding pressure profiles for the two cases. Combining the density and pressure profiles we can calculate the local velocity of sound. This is done in the sequel.

The exercise of providing some independent checks on the numerical computations is carried out in section 3.3. We first set up a comparison with the calculations of Su *et al* [14]. This is made possible by using an explicit expression for $n_0(\boldsymbol{r})$, derived by Chou *et al* [17] by calculating the density matrix. The fugacity values are compared in table 1 for $N = 40\,000$ and $a/a_0 \approx 0.007$. The agreement between the values is excellent. The density profiles obtained by the two methods are drawn in figure 6 for comparison. The agreement is excellent, except for $\tau = 35$ (which is close to τ_C) for r/a_0 below 2.5.

Another check on the computations is provided by the calculation of τ_C. It can be estimated by locating the point $x_D = 0$ on the temperature axis of the x_D–τ plot. These plots are shown in figures 7 and 8 for (i) $N = 10^4, a/a_0 = 0.001$ and (ii) $N = 40\,000, a/a_0 \approx 0.007$, respectively. This method yields values $\tau_C = 20.4$ and $\tau_C = 30.6$, respectively for the two cases. These compare well with the values calculated from the critical line given by (26), as is evident from table 2. The values calculated using a recent expression for T_C derived by Kao and Jiang [18] are also included in table 2.

In the earlier sections a numerical scheme was presented to study the properties of a weakly repulsive interacting collection of bosons trapped in a harmonic potential. Section 3.4 looks at the same system in a BHP to delineate the combined effect of a finite size and

interactions. To illustrate the general principles x_0 is fixed at 100 and the scheme of section 3.3 is adapted to the case of a BHP. We choose $N = 40\,000$ and $a/a_0 \approx 0.007$ and calculate x_D for various values of τ. As expected on physical grounds, the condensate radius increases with confinement. For example, for $\tau = 25$, x_D increases from 14.891 to 17.912. The comparison can be seen in figure 13.

The density and pressure profiles can be plotted by employing the relevant formulae with the indicated modifications. These are presented in figures 9 and 10, respectively for $\tau = 25$. These profiles have been compared with those plotted for an unbounded harmonic oscillator potential.

The dimensionless velocity of sound c' obtained from (52) has been tabulated in table 3 and depicted graphically in figure 11. The phonon like excitations known as Bogoliubov sound are obtained for $\lambda \gg \xi$, where λ is the wavelength of the excitations and $\xi = \sqrt{8\pi a n_0}$ (n_0 being the condensate density) is the healing length. Experimentally, sound waves in Bose–Einstein condensed gases are generated by focusing a laser pulse on the centre of the trap. The subject of the various possible modes of oscillation is of great interest [8, 20].

We have also computed the condensate fraction N_0/N for the case $N = 40\,000$ for both the ideal and a weakly repulsive Bose gas ($a/a_0 \approx 0.007$) in a BHP with $x_0 = 100$. All the results are plotted in figure 12. It is evident from the figure that the condensate fraction increases when the system is confined to a small region. The depletion of the condensate in the presence of repulsion between bosons is another feature which can be clearly seen. A very detailed analysis of the condensate fraction has been recently carried out by F Gerbier *et al* [22] and, Davis and Blakie [23].

Acknowledgments

Sonia Lumb expresses her gratitude to the Council of Scientific and Industrial Research (CSIR) for the financial assistance for carrying out this project. The authors are thankful to the head of the Department of Physics and Astrophysics, University of Delhi for providing the necessary facilities to carry out this work. They are also grateful to Professor K K Singh for illuminating discussions.

References

[1] Bogoliubov N N 1947 *J. Phys. USSR* **11** 23
[2] Huang K, Yang C N and Luttinger J M 1957 *Phys. Rev.* **105** 776
[3] Beliaev S T 1958 *Sov. Phys.—JETP* **7** 289
Beliaev S T 1958 *Sov. Phys.—JETP* **7** 299
[4] Popov V N 1987 *Functional Integrals and Collective Excitations* (Cambridge: Cambridge University Press)
See also Griffin A 1996 *Phys. Rev.* B **53** 9341
[5] Andersen J O 2004 *Rev. Mod. Phys.* **76** 599
[6] Gross E P 1963 *J. Math. Phys.* **4** 195
[7] Pitaevskii L P 1961 *Sov. Phys.—JETP* **13** 451
[8] Pitaevskii L and Stringari S 2003 *Bose–Einstein Condensation* (Oxford: Oxford University Press)
[9] Pethick C J and Smith H 2002 *Bose–Einstein Condensation in Dilute Gases* (Cambridge: Cambridge University Press)
[10] Dalfavo F, Giorgini S, Pitaevskii L P and Stringari S 1999 *Rev. Mod. Phys.* **71** 463
[11] Giorgini S, Pitaevskii L P and Stringari S 1997 *J. Low Temp. Phys.* **109** 309
[12] Shi H and Zheng W 1997 *Phys. Rev.* A **56** 2984
[13] Oliva J 1989 *Phys. Rev.* B **39** 4197
[14] Su G, Chen L and Chen J 2004 *J. Phys. A: Math. Gen.* **37** 3041
[15] Lumb S, Muthu S K and Singh K K 2006 *Int. J. Mod. Phys.* B **20** 151
[16] Singh K K 1967 *Physica* **34** 285

[17] Chou T T, Yang C N and Yu L H 1996 *Phys. Rev.* A **53** 4257
[18] Kao Y M and Jiang T F 2006 *Phys. Rev.* A **73** 043604
[19] Lumb S and Muthu S K 2003 *Int. J. Mod. Phys.* B **17** 5855
[20] Stamper-Kurn D M, Miesner H-J, Inouye S, Andrews M R and Ketterle W 1998 *Phys. Rev. Lett.* **81** 500
[21] Lumb S and Muthu S K 2001 *Int. J. Mod. Phys.* B **15** 2169
[22] Gerbier F, Thywissen J H, Richard S, Hugbart M, Bouyer P and Aspect A 2004 *Phys. Rev.* A **70** 013607
[23] Davis M J and Blakie P B 2006 *Phys. Rev. Lett.* **96** 060404